JOURNAL OF Applied Polymer SCIENCE

Poly(amino ether)/Organoclay Nanocomposites: Preparation and Characterization

Ainhoa Granado, Jose Ignacio Eguiazábal
Dpto. de Ciencia y Tecnología de Polímeros and Instituto de Materiales Poliméricos 'POLYMAT', Facultad de Química UPV/EHU, PO Box 1072, 20080, SAN SEBASTIÁN, Spain
Correspondence to: J. I. Eguiazábal (E-mail: josei.eguiazabal@ehu.es)

ABSTRACT: Dispersed polymer nanocomposites based on a poly(amino ether) resin and organically modified laminar clays were obtained. The chemical nature of the organic modifier of the clay and the processing temperature were first chosen using Young's modulus of the nanocomposites as a measure of the dispersion level. The Cloisite® 20A organoclay and a processing temperature of 170°C were the fixed parameters. Additionally, the clay content of the nanocomposites was changed and their nanostructure and properties were measured. A significant increase in the modulus of elasticity (35% with 4.3% montmorillonite addition) was observed, together with an unusual increase in ductility. The ductility behavior is attributed to a high degree of confinement of polymer chains inside the silicate layers, and the modulus values are discussed taking into account not only the dispersion level, but also the length of the clay particles. © 2014 Wiley Periodicals, Inc. J. Appl. Polym. Sci. **2015**, *132*, 41239.

KEYWORDS: clay; mechanical properties; molding; morphology; property; structure

Received 4 February 2014; accepted 29 June 2014
DOI: 10.1002/app.41239

INTRODUCTION

Polymeric nanocomposites (NCs) have been the object of great academic and industrial attention in recent years in the search for light weight and high-performance materials. In particular, polymers filled with small amounts of organically modified layered silicates dispersed at the nanoscale level combine the advantages of organic polymers (light weight, versatility, good moldability) and inorganic fillers (high stiffness and strength, thermal stability and chemical resistance).[1] Moreover, negative effects (increased density, loss of transparency) as compared with those present in microcomposites, are limited.[1] Among the methods used to prepare NCs, the three most commonly used are in situ polymerization, solvent intercalation and melt intercalation.[2,3] *In situ* polymerization and solvent methods are interesting from a scientific standpoint. However, melt processing is the most widely used production method for NCs based on thermoplastics polymers as it can be carried out in conventional industrial polymer processing machinery without any problem from organic solvents or monomers.

It is well known that optimum properties of nanoclay-based NCs are obtained when an exfoliated or highly dispersed nanostructure is obtained[4] because the modulus of elasticity is very sensitive to the dispersion level. Therefore when dispersion is limited,[5–10] the modulus increase is moderate. For this reason, ascertaining which parameters lead to good dispersion is a subject of obvious interest. The first of the key parameters in this regard is the processing conditions,[11,12] and second, the chemical structure of the alkyl ammonium compound used to modify the clay so as to achieve favorable interactions between the modification of the clay and the polymer matrix.[13–16] Thus, organoclays with one long alkyl group lead to better exfoliation than those with two long alkyl groups and two methyl groups give rise to higher modulus than two hydroxyl-ethyl groups substituents in nylon 6 based NCs.[13] The use of alkyl ammonium cations with chain lengths longer that eight carbons and clays with low to intermediate charge density led to greater exfoliation in epoxy-based NCs.[15] However, in polypropylene-based NCs the chain lengths must be longer than 12 carbons to promote exfoliation in conjunction with maleated polypropylene[16] and in polyethylene-based NCs, organoclays with two alkyl tails are superior to the organoclays with one alkyl tail in terms of clay dispersion and mechanical improvement. This indicates that, it is not possible to make generalizations based on these results about the relationship between organoclay structure and NC morphology.

In addition to the factors indicated in the previous paragraph, the structural characteristics of the layered silicate may further influence nanocomposite morphology.[15,17–20] The level and distribution of cationic exchange sites and the average size of the platelet stacks and of the individual platelets that comprise them are among the structural variables that may affect the

extent of clay dispersion and the final particle size and consequently the properties of polymer–clay NCs. Thus, for example, Yano et al.[18] compared the properties of polyimide based NCs with clays of different lengths, and concluded that the degree of improvement of the properties clearly depends on particle length. The results show that the largest clay, i.e., mica, is the most effective at reducing the gas permeability coefficient and at increasing the elastic modulus (from about 2300 MPa to 3400 MPa for NCs based on a clay with 460 Å and 12300 Å of length, respectively).

As has been reported in the literature,[4,21–23] different studies of NCs based on polymers with single lateral hydroxyl groups (epoxy, phenoxy, and EVOH) have been carried out. This is due to the possibility of interaction or reaction with other polar functional groups that could in turn facilitate interaction with clays and consequently improve clay dispersion or exfoliation. Thus, EVOH was blended with a modified clay (Nanomer® I.35L) containing 30–40% polyoxyethylene decyloxypropylamine.[4] The blending conditions influenced the clay morphology, and the modulus and yield strength increased. Phenoxy was blended[21] with clays modified with dimethyl dehydrogenated tallow quaternary ammonium (Cloisite® 20A), methyl tallow bis2-hydroxyethyl quaternary ammonium (Cloisite® 30B) and octadecylamine (OCT). There was a modulus increase of 45% with 4% montmorillonite (MMT) Cloisite® 30B and 33% with Cloisite® 20A. The dispersion in EVOH and phenoxy based NCs was tentatively attributed to chemical interactions between the hydroxyl groups of these polymers and the oxygen atoms of the clay forming hydrogen bonds.

Poly(amino ether) resins (PAE) are a family of thermoplastics characterized by very good barrier properties, excellent adhesion to different substrates, high optical clarity, low color, and good toughness.[24] Their potential applications are mainly in the packaging industry. This polymer has a chemical structure characterized by the presence of three lateral hydroxyl groups per repeating unit on the main chain. In NCs of PAE resins with functionalized multi-walled carbon nanotubes,[22,23] the functionalization greatly improved dispersion and the thermal and mechanical properties, particularly the latter: the modulus increased by 65% and the tensile strength by 60% compared with those of the pure polymer when 2% nanotubes were added. However, to our knowledge, the PAE used in this work has not yet been studied as a matrix for organoclays- or nanotubes-based NCs.

Because of the lack of available information on the behavior of PAE based NCs, in this work, new NCs based on a PAE resin were studied. They were obtained in the melt state since the shear stress that takes place in the extruder aids dispersion and exfoliation of the nanoclays. Initial work was carried out to select the best organoclay from three commercial organoclays with different volume and polarity of the surfactant. This was done using the modulus of elasticity as the parameter for selecting the best dispersed organoclay on the NCs filled with 5% of each organoclay since the modulus of elasticity is known to be directly related to dispersion in MMT based polymer NCs.[13,17,25] NCs based on the selected clay were prepared with different clay contents and characterized by dynamic–mechanical analysis (DMA), X-ray diffraction and TEM, and tensile stress–strain tests. The results are discussed and compared with those of previous works.

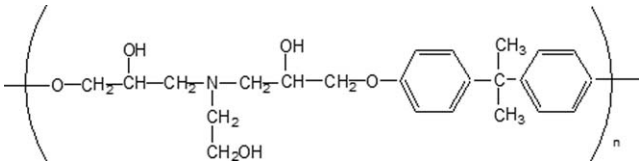

Figure 1. Chemical structure of the poly(amino ether) resin.

EXPERIMENTAL

Materials

The PAE resin was kindly supplied by Dow Chemical. Its chemical structure is shown in Figure 1. It had a melt flow index (MFI) of 9 g 10 min^{-1}, measured at 200°C and with 2.16 kg load. The nanofillers were three organically-modified montmorillonites. The first organoclay (Cloisite® 20A, Southern Clay Products) used dimethyl dehydrogenated tallow quaternary ammonium as the surfactant. The second one (Nanomer® I.30 TC, Nanocor) used octadecylamine. The third modification was bis-2-hydroxyethyl methyl tallow quaternary ammonium (Cloisite® 30B, Southern Clay Products). Drying before processing was performed at 65°C in an air-circulation oven for 6 h for PAE, and at 80°C for 4 h in the case of the clays.

Processing

The PAE-based NCs with 5 wt % of the three organoclays were first prepared in a Collin ZK25 corotating twin-screw extruder-kneader (screw diameter of 25 mm and *L/D* ratio= 30) at 170 and 200°C with the aim of optimizing the processing temperature. The rotation speed was 200 rpm. After extrusion, the extrudates were cooled in a water bath and pelletized. Subsequent injection molding was carried out in a Battenfeld BA-230E reciprocating screw injection molding machine and tensile (ASTM D638, type IV, thickness 2.05 mm) specimens were obtained. The screw of the plasticization unit was a standard screw with a diameter of 18 mm, *L/D* ratio of 17.8 and a compression ratio of 4. The melt temperature was 185°C and the mold temperature 15°C. The injection speed and pressure were 10.2 cm^3 s^{-1} and 2600 bar, respectively. The PAE/Cloisite® 20A NCs, which showed a slightly higher modulus increase, were prepared in the extruder at 170°C with clay contents ranging from 1 to 7 wt %. The rest of the processing methods and conditions were identical to those previously reported. The real amount of MMT in the NCs, i.e., without the organic modifier, was measured weighing the remaining mass (MMTash) relative to the original NC mass, after calcination at 900°C for 45 min, by means of:

$$\%MMT = \%MMTash/0.942 \quad (1)$$

Dynamic Mechanical Analysis

Dynamic mechanical analysis was performed using a TA Q800 DMA that provided the loss tangent (tan δ) and the storage modulus (E') against temperature. The scans were carried out in bending mode at a constant heating rate of 4°C min^{-1} and at a frequency of 1 Hz, from 30 to roughly 120°C. The glass

transition temperature (T_g) was measured as the temperature at the maximum of the tan δ plots.

Nanostructure

X-ray diffraction patterns were recorded on a Bruker D8 diffractometer operating at 45 kV and 50 mA, using a Ni-filtered CuKα radiation source ($\lambda = 0.15406$ nm). The transmission electron microscopy (TEM) samples were ultrathin-sectioned at 150−200 nm using an ultramicrotome. The micrographs were obtained in a Philips Tecnai G2 20 Twin microscope at an accelerating voltage of 200 kV and analyzed by means of an image analysis program (Scion Image) which accounts for the particle thickness and length on the image files. Dispersed platelets and/or agglomerates were printed on a transparency film using a black permanent marker pen. Agglomerates and intercalated structures were treated as single particles. The resulting transparency was scanned and converted into an image file.

Orientation

The birefringence of the injection molded tensile specimens was measured at room temperature using an Olympus BX40 polarized light microscope equipped with a compensator. Each birefringence value was obtained from a minimum of three measurements.

Tensile Tests

Tensile testing was carried out using an Instron 5569 machine, at a cross-head speed of 10 mm min^{-1}, at 23 ± 2°C and 50 ± 5% relative humidity. The mechanical properties (yield stress and ductility, measured as the break strain) were determined from the load-displacement curves. Young's modulus was determined by means of an extensometer (Instron 2630-102 Static Extensometer, Gauge Length 10 mm) at a crosshead speed of 1 mm min^{-1} to obtain more accurate values. A minimum of five tensile specimens were tested for each reported value.

RESULTS AND DISCUSSION

Melt Temperature and Organoclay for the Best Dispersion

It is known that the dispersion level and, consequently, the properties of NCs based on a fixed matrix are primarily influenced, among others, by the chemical nature of the organic modification of the clay,[12–14] and by the melt processing conditions.[11,12] For this reason, a preliminary study was carried out to fix these two parameters at values that should lead to the best dispersion. The modulus of elasticity was used to assess dispersion because (i) it is directly related to the dispersion level,[13,17,25] (ii) it is easy to measure and, mainly, (iii) it is a bulk parameter, much less local than the results of either WAXD or TEM analysis that anyway can serve to complement this preliminary study.

The moduli of elasticity of the NCs after the addition of 5% of each organoclay and processing at 170 and 200°C are shown in Figure 2. 170°C is the minimum processing temperature for PAE, and 200°C is the maximum recommended temperature for organoclays in order to minimize their degradation.[26] As can be seen, whatever the nature of the organoclay, processing at 170°C always led to slightly higher modulus values. Given previous findings,[13,27] it would appear that the higher modulus values obtained at lower temperature (170°C) are the result of the higher melt viscosity and consequently higher shear stress obtained at this temperature, which favors dispersion and exfoliation of the organoclay layers. In this way, a slightly higher temperature would not improve modulus. Consequently, 170°C was selected as the processing temperature for the following full characterizing study of the PAE-based NCs of this work.

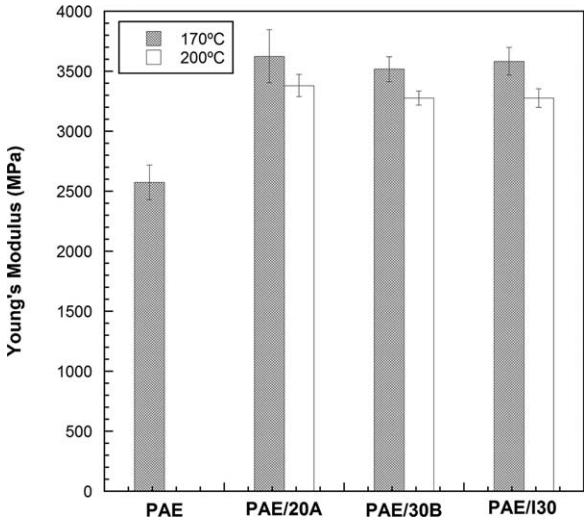

Figure 2. Young's modulus of PAE-based NCs with different clays processed at 170 and 200°C.

With respect to the fitting of the chemical nature of the organoclay, in an attempt to adequate the chemical modification to the PAE matrix, the chemical characteristics of PAE should be taken into account. From the viewpoint of interaction with other components, the most relevant characteristics are the three pendant hydroxyl groups of the main chain (Figure 1). Due to this polarity, and looking to the possibility of interaction, polar modifiers such as that of the Cloisite® 30B organoclay, which has hydroxyl groups, appear adequate. The chosen second organoclay was Nanomer® I30 because it is claimed that this clay is designed for ease of dispersion into amine-cured epoxy resins,[4] which are chemically similar to PAE. Finally, Cloisite® 20A was also chosen because, in spite of the less polar nature of its modification, it has led to favorable results with polar polymers such as phenoxy.[13,28] As a whole, these three organoclays have the same amount of substituted molecules, but they differ in the volume and polarity of the surfactant. Moreover, the higher volume of the molecules of the surfactant of 20A leads to a lower exposed inorganic content for the same overall content of organoclay.

As the MMT content of the three OMMTs in this study is different, to be able to compare their increases in modulus, the moduli of elasticity of the NCs with 5% of each OMMT produced at 170°C are shown in Figure 3 versus their MMT content. The MMT content of each OMMT was calculated as indicated in the experimental section. Young's modulus values are extrapolated to 0% OMMT. As can be seen, the modulus increases for I30 and 30B reinforced NCs were similar (38.9 and 36.4%, respectively). The modulus of the NC with the 20A organoclay is slightly higher (40.6%). The increase for the

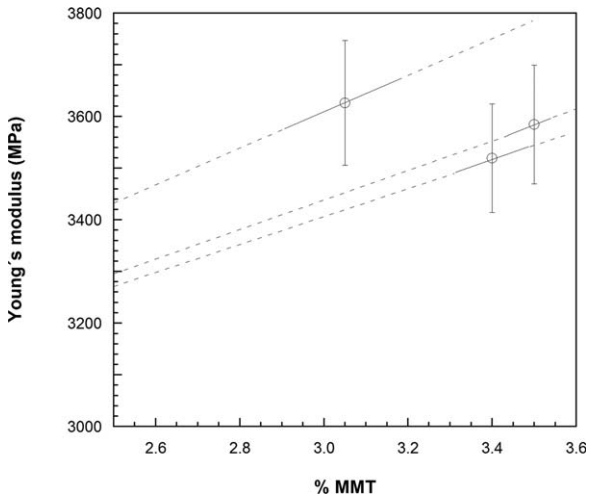

Figure 3. Young's modulus of PAE-based NCs processed at 170°C (○) versus MMT content.

interlayer distance (Δd_{001}) of the three NCs, determined by WAXD, was also similar (0.90 nm for PAE/20A and PAE/30B and 0.82 nm for PAE/I30 NCs). However, as can be seen in Figure 3, the 20A organoclay has a lower inorganic content than either I30 or 30B. Extrapolating the modulus value of the NC with 20A organoclay to the same inorganic contents as those of the NCs with 30B or I30, a value of roughly 3760 MPa was obtained, which was clearly the highest. Moreover, as can be seen in Figure 4, TEM analysis also seemed to reflect a slightly better dispersion for PAE/20A NCs. For this reason the Cloisite® 20A organoclay and a processing temperature of 170°C were chosen to conduct the subsequent research.

Characterization

Before examining the nanostructure, a possible effect of the clay presence on the T_g of PAE was studied. The tan δ results obtained by DMTA are shown in Figure 5. The storage modulus (E') results will be discussed later. The T_g of the NCs, measured at the maximum of the tan δ plots (78°C), clearly increased with respect to that of the neat PAE (69°C), and a slight tendency to increase with MMT concentration was also observed. The increase in T_g after the addition of the organoclay is due to interactions between the polymer and the inorganic filler particles[29] and the restricted mobility of the segments that this causes in the vicinity of the organoclay. A T_g increase has been commonly reported,[30–32] although a decrease in the T_g of the matrix in presence of organoclay, consequence of the migration of the surfactant during melt mixing,[33–36] or even a constant T_g[37–39] have also been observed.

The nanostructure of the NCs was characterized both by WAXD and TEM. It is known that WAXD results reveal intercalation; this is because exfoliation cannot be concluded from the absence of a diffraction peak, as it can occur through a non-constant basal spacing, for instance.[14] In Figure 6, the WAXD scans of the NCs with different MMT contents, as well as that of the neat Cloisite® 20A are shown. As can be seen, the scan of Cloisite® 20A shows the peak characteristic of the (001) plane at a diffraction angle of 3.89° which, according to Bragg's law, corresponds to a basal distance, d_{001}, of 2.27 nm. The main peak of the NCs appeared at 2.78° whatever the MMT content (basal distance 3.17 nm). This basal distance increase ($\Delta d_{001} = 0.90$ nm) is similar to those obtained in NCs based on phenoxy ($\Delta d_{001} = 0.90$ nm),[21] poly(ethylene terephthalate) ($\Delta d_{001} = 0.92$ nm)[2] and PCTG ($\Delta d_{001} = 0.89$ nm)[40] and slightly higher than those obtained in EVOH and PVOH ($\Delta d_{001} = 0.70$ nm) based NCs.[1,4] This result indicates that PAE intercalates inside the galleries of the organoclay. As this Δd_{001} is similar to the thickness of the clay layers, the volume of the particles roughly doubled after intercalation.

Figure 7(a–c) show representative TEM micrographs of the NCs with 2, 5, and 7% organoclay, corresponding to MMT contents of 1.2, 3.0, and 4.3%, respectively. The corresponding particle length and thickness, and the number of platelets per particle are shown in Table I. The number of particles measured was roughly 200 per composition. As can be seen, the organoclay is homogeneously dispersed in the matrix. The particles usually contain 4–6 platelets indicating difficult exfoliation. A similar dispersion level with mainly intercalated nanostructure has also been observed in PET-based NCs[2] or in NCs with other matrices with similar chemical characteristics such as EVOH[4] or phenoxy.[21] In the case of EVOH-based NCs, additional techniques were used to ameliorate exfoliation[4,41] such as the addition of

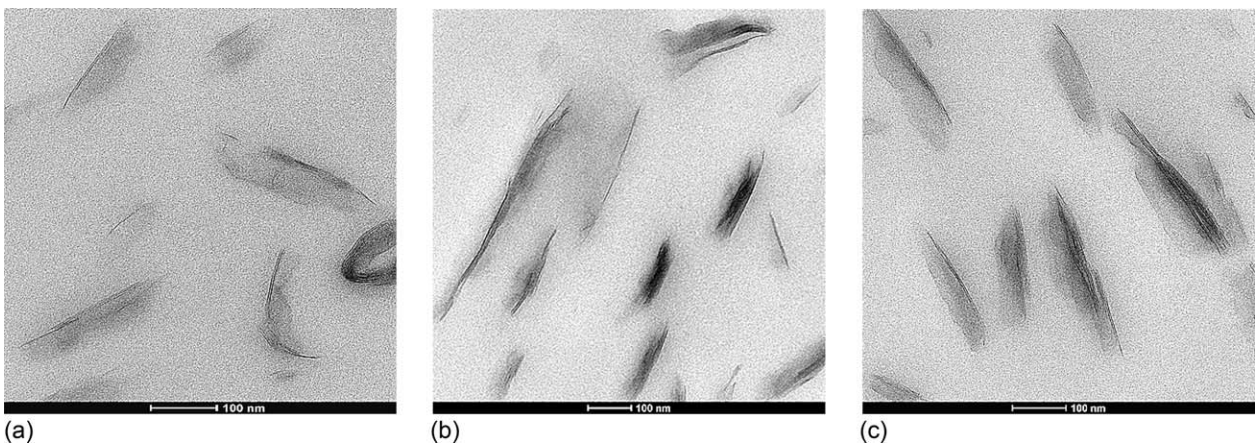

Figure 4. TEM photomicrographs of the 95/5 (a) PAE/20A, (b) PAE/I30, and (c) PAE/30B NCs.

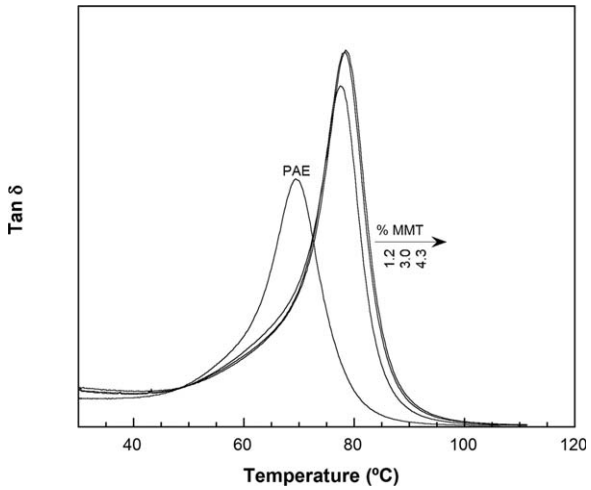

Figure 5. Tan δ-temperature data for PAE/20A NCs.

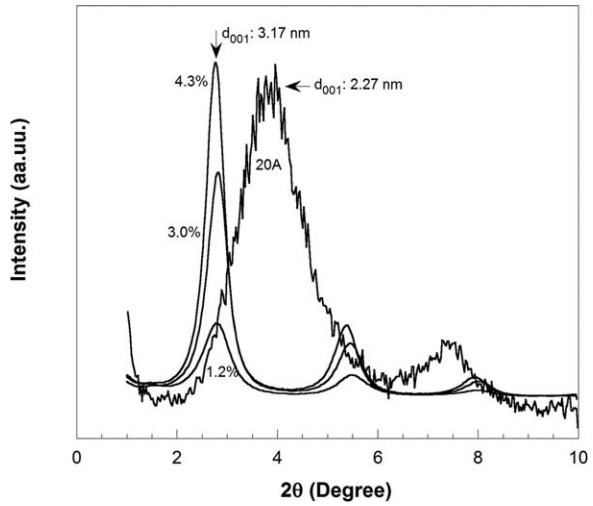

Figure 6. WAXD patterns of the PAE/20A NCs and Cloisite® 20A organoclay.

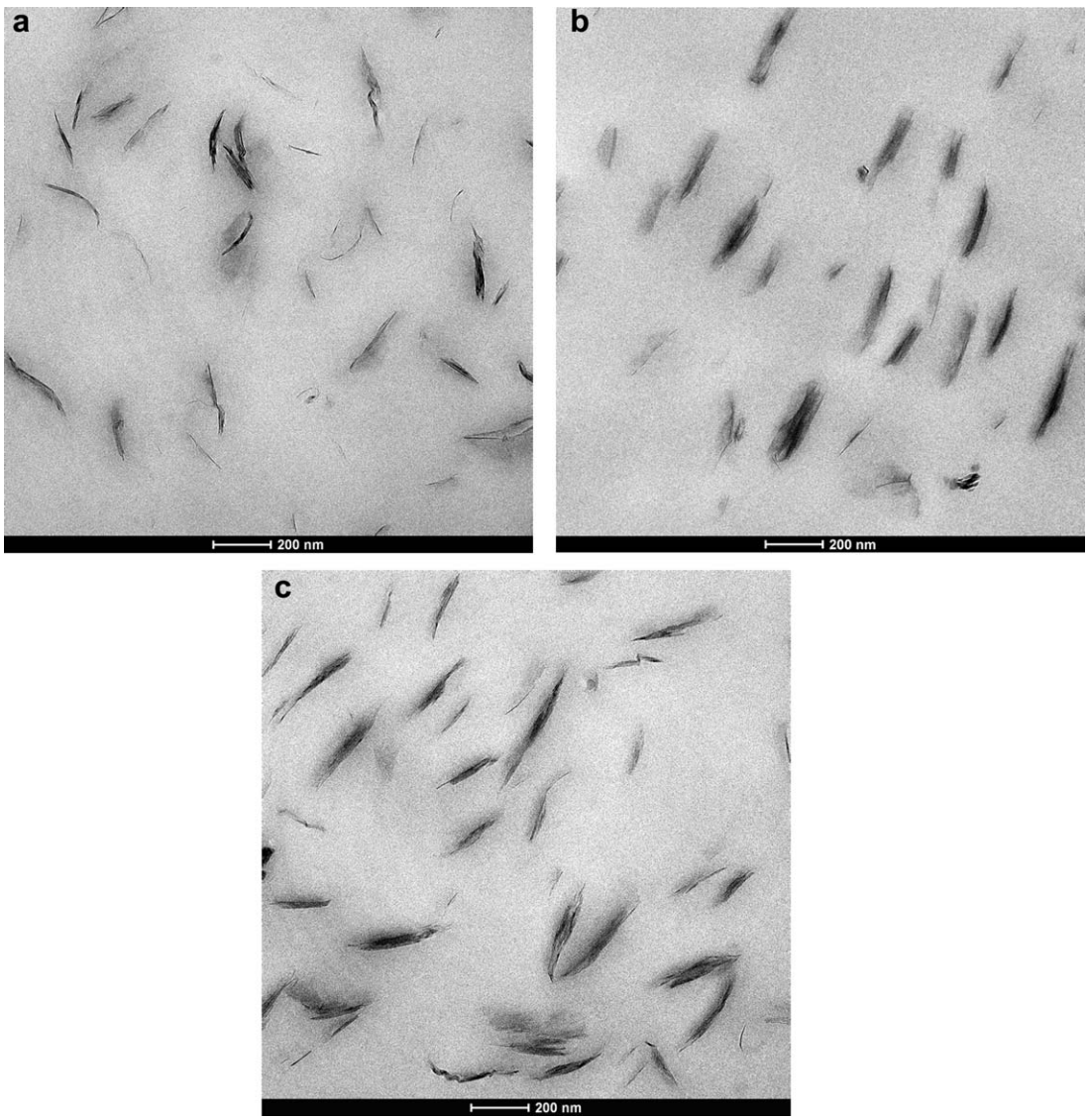

Figure 7. TEM photomicrographs of the PAE/20A NCs with (a) 1.2, (b) 3.0, and (c) 4.3% MMT at high magnification.

Table I. Image Analysis Results of the TEM Micrographs

	1.2% MMT	3.0% MMT	4.3% MMT
Particle length, l_n (nm)	66	100	124
Particle thickness, t_n(nm)	11.5	14.8	18.2
Number average Platelets per particle	3.7	4.5	6.1

polymers (PA6) or compatibilizers (EVA-*g*-MA or LLDPE-*g*-MA) with polar groups. Any of these techniques are possible ways to test additional dispersion in these NCs.

As can also be seen, the particle length and thickness increased greatly with the MMT content. Thickness increases occur at high MMT contents.[42–44] The number of stacks present initially in the melt should not influence dispersion. However, in this case unexpectedly this effect appeared as seen in Figure 7 and quantitatively measured on Table I.

Similarly to this work (Figure 7 and Table I), a large increase in thickness was observed in amorphous polyamide based NCs (from 4.2 nm with 1.6% MMT to 9.3 nm with 5.5% MMT).[42] Moreover, as observed in some compatibilized NCs,[43–45] particle thickness is closely related to dispersion level, since it clearly increases as the dispersion worsens.

The particle thickness increase indicates that the number of sheets per particle increased because Δd_{001} was independent of the MMT content. A second relevant feature is that, although many sheets did not fully separate from each other leading to exfoliation, they largely slipped from each other.[19,45,46] This is indicated by the increase in length of the particles which is especially pronounced at high clay contents: the length in the 4.3% MMT NC (124 nm) is twice that of the 1.2% NC (66 nm). Therefore, in this system, the thick morphology of the particles is not necessarily negative, because it leads to greater length. Thus, these thick particles give rise to almost twice the external surface and, therefore, contact area, which should influence the mechanical properties.

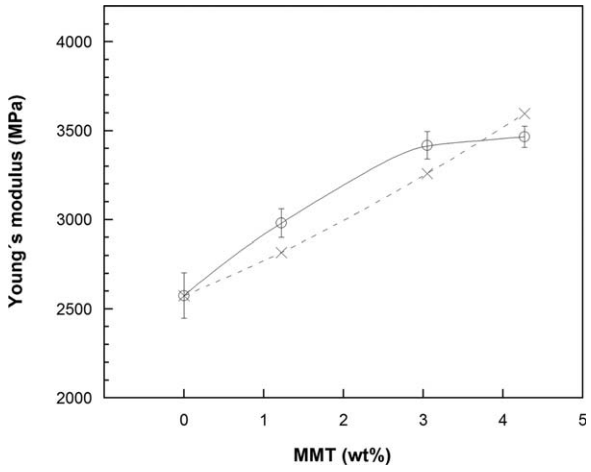

Figure 8. Experimental (○) and Halpin-Tsai (x) Young's modulus of the PAE/20A NCs versus MMT content.

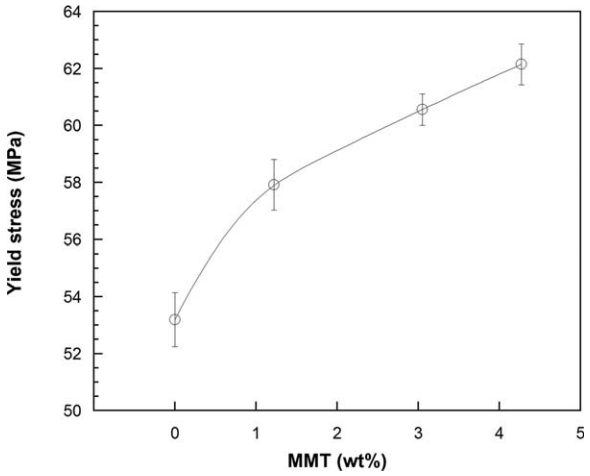

Figure 9. Yield stress of the PAE/20A NCs versus MMT content.

Mechanical Properties

Figure 8 shows the modulus of elasticity of the NCs, as a function of the MMT content. The yield stress values (Figure 9) exhibited as usual similar behavior[21,42,46,47] being their increases proportionally lower than those of the modulus; i.e., from 53 MPa to 62 MPa when the MMT content increased from 0 to 4.3%. Similar increases have been obtained in phenoxy/20A NCs (when the MMT content increased from 0 to 3.9%).[21] The experimental Young's moduli of the NCs (E) are compared in Figure 8 with those obtained from the Halpin-Tsai composite model [eq. (2)] usually applied for nanocomposites. The Halpin-Tsai equation is as follows:

$$\frac{E}{E_m}=\frac{1+2(l/t)\eta\phi_f}{1-\eta\phi_f},\ \eta=\frac{E_f/E_m-1}{E_f/E_m+2(l/t)} \tag{2}$$

l: filler length E_f: modulus of the filler (178 GPa)[43]

t: filler thickness E_m: modulus of the matrix (2.58 GPa)

ϕ_f: filler volume fraction

The filler and the matrix have to be linearly elastic, isotropic and firmly bonded[19] and the filler has to be aligned and uniform in shape and size. In this study, any possible effect of orientation on the modulus should be low, due to the greater effect caused by the inorganic reinforcement. Moreover, the filler particles (Figure 7) were almost fully oriented in the flow and testing direction. Average filler length and thickness values were used. It can be observed in Figure 8 that using this model, the correlation between experimental and predicted moduli is fairly good, since the maximum difference between them is about 150 MPa. Although, as in this work, higher than predicted values have also been observed in NCs with thick particles,[19,44,46,48] the predicted values are usually higher than the experimental ones.[19,47]

If we look at the modulus increase at 3% MMT for instance, it reached 32%. This is similar to that obtained in phenoxy (30% with 3% MMT)[21] and PCTG-based NCs (32% with 3% MMT)[40] and higher than that of PET-based NCs (20% with 3% MMT).[2] However, the most relevant feature is that in these nanocomposites with 4–6 layers per particle, and therefore with

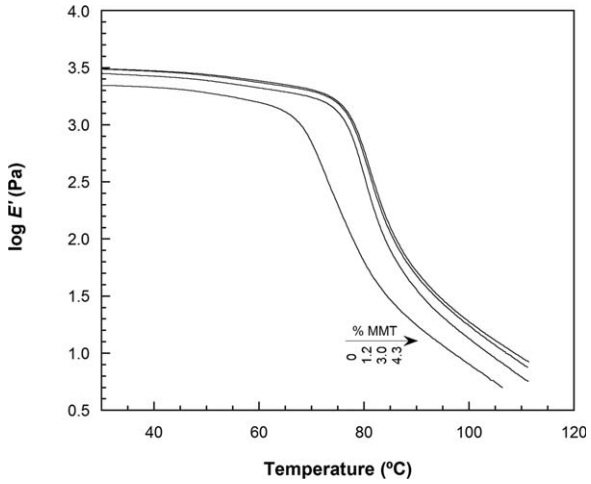

Figure 10. Storage modulus, E'-temperature data for PAE/20A NCs.

low dispersion, the modulus increases are high. The contact area of the NCs in this study appears to be 4–6 times smaller than in NCs with almost full dispersion (almost 1 layer per particle), such as PA6-based NCs, or NCs with dispersion levels similar to those obtained in amorphous polyamide based NCs (1.4 layer per particle). However, the modulus increases of PAE-based NCs are far from being smaller in the same proportion than those of PA6 or aPA NCs where the modulus increases were 40% and 36% respectively at the same MMT content.[13,42] Therefore, ruled out a potential influence of molecular orientation, because the birefringence and thus the orientation were independent of the MMT content, the observed increases of this study hardly correspond to those could be expected from the dispersion measured by the number of sheets per stack. However, as observed in Figure 7 and Table I, the increase in length in these NCs is unusually large[42,46,49] leading to a contact area almost double than when dispersion only measured by the number of sheets per particle is considered. In another previous system both the increase in length and the consequent increase in modulus were small.[17]

Thus, high length of clay particles is proposed as the reason for the rather high modulus increase observed in this study, that did not correspond in a first approximation with the limited dispersion level observed.

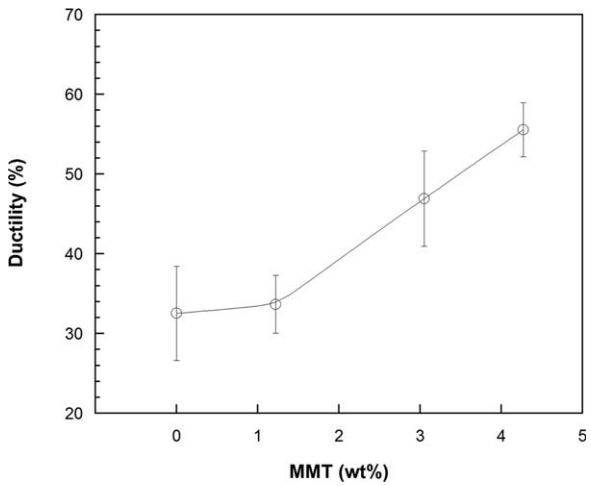

Figure 11. Ductility of the PAE/20A NCs versus MMT content.

Moreover, as seen in Figure 10, where the storage modulus, E', is shown against temperature, the increase with the MMT content also occurred at higher temperatures thanks to the rigid nature of the MMT that extends the reinforcing effect up to the glass transition temperature of the PAE matrix.

The ductility of the NCs, measured by means of the elongation at break, is shown in Figure 11. As can be seen, the ductility remained constant when small amounts of MMT were added (1.2%) and, unexpectedly because of the rigid nature of the filler, it increased at higher MMT contents. This is unusual in most NCs,[1,13,42,44,47,50] although ductility increases have also been reported,[51–53] among others in phenoxy based NCs, where increases of 22% and 43% were obtained with the addition of 4.1% of Cloisite® 30B and 3.9% of Cloisite® 20A organoclay, respectively.[21,28] These ductility increases are not due to the migration of interlayer surfactant to the polymeric matrix during processing and the consequent plasticizing effect,[28] because the T_g of PAE did not decrease when the nanoclay was added. Therefore, they are tentatively attributed[52,53] to surfactant/polymer interactions within the clay galleries, giving rise to a higher confinement of polymer chains inside the silicate layers. This is in agreement with the high Δd_{001} values observed and would lead to higher energy-dissipation mechanism in the NCs, delaying the crack formation.

CONCLUSIONS

A processing temperature of 170°C and the Cloisite® 20A organoclay led to the best dispersion in the PAE matrix on the basis of a preliminary study on the modulus of elasticity. Nanoclay dispersion was not very wide and the particle thickness increased with the MMT content; however, most sheets in the nanoparticles largely slipped from each other leading to an increase in length.

The modulus increases obtained reached 32% with only 3% MMT, higher than what could be expected given the dispersion level; therefore, it is proposed that the length of the clay particles has to be taken into account, together with the dispersion level, when the modulus values are discussed. Ductility improved after nanoclay addition due to surfactant/polymer interactions.

ACKNOWLEDGMENTS

The financial support of the Basque Government (Projects IT611-13 and S-PE11UN050) and of the University of the Basque Country (UFI11/56) is gratefully acknowledged.

REFERENCES

1. Chang, J.-H.; Jang, T.-G.; Ihn, K. J.; Lee, W.-K.; Sur, G. S. *J. Appl. Polym. Sci.* **2003**, *90*, 3208.
2. Gurmendi, U.; Eguiazábal, J. I.; Nazábal, J. *Macromol. Mater. Eng.* **2007**, *292*, 169.

3. Kato, M.; Usuki, A. In: Polymer-Clay Nanocomposites; Pinnavaia, T. J.; Beall, G. W., Eds.; Wiley: New York, **2001**; Chapter 5.
4. Artzi, N.; Narkis, M.; Siegmann, A. *J. Polym. Sci. Polym. Phys.* **2005**, *43*, 1931.
5. Liu, X.; Wu, Q. *Macromol. Mater. Eng.* **2002**, *287*, 180.
6. Kim, J. H.; Koo, C. M.; Choi, Y. S.; Wang, K. H.; Chung, I. J. *Polymer* **2004**, *45*, 7719.
7. Huang, J. C.; Zhu, Z. K.; Yin, J.; Qian, X. F.; Sun, Y. Y. *Polymer* **2001**, *42*, 873.
8. Su, S.; Jiang, D. D.; Wilkie, D. A. *Polym. Degrad. Stab.* **2004**, *83*, 321.
9. Sánchez-Solís, A.; Romero-Ibarra, I.; Estrada, M. R.; Calderas, F.; Manero, O. *Polym. Eng. Sci.* **2004**, *44*, 1094.
10. Mishra, J. K.; Chang, Y. W.; Choi, N. S. *Polym. Eng. Sci.* **2007**, *47*, 863.
11. Lertwimolnun, W.; Vergnes, B. *Polym. Eng. Sci.* **2006**, *46*, 314.
12. Zhu, L.; Xanthos, M. *J. Appl. Polym. Sci.* **2004**, *93*, 1891.
13. Fornes, T. D.; Yoon, P. J.; Hunter, D. L.; Keskkula, H.; Paul, D. R. *Polymer* **2002**, *43*, 5915.
14. Fornes, T. D.; Hunter, D. L.; Paul, D. R. *Macromolecules* **2004**, *37*, 1793.
15. Lan, T.; Kaviratna, P. D.; Pinnavaia, T. J. *Chem. Mater.* **1995**, *7*, 2144.
16. Reichert, P.; Nitz, H.; Klinke, S.; Brandsch, R.; Thomann, R.; Mulhaupt, R. *Macromol. Mater. Eng.* **2000**, *275*, 8.
17. Fornes, T. D.; Hunter, D. L.; Paul, D. R. *Polymer* **2004**, *45*, 2321.
18. Yano, K.; Usuki, A.; Okada, A. J. *J. Polym. Sci. Part A, Polym. Chem.* **1997**, *35*, 2289.
19. Fornes, T. D.; Paul, D. R. *Polymer* **2003**, *44*, 4993.
20. Usuki, A.; Koiwai, A.; Kojima, Y.; Kawasumi, M.; Okada, A.; Kurauchi, T.; Kamigaito, O. *J. Appl. Polym. Sci.* **1995**, *55*, 119.
21. Gurmendi, U.; Eguiazábal, J. I.; Nazábal, J. *Comp. Sci. Tech.* **2006**, *66*, 1221.
22. Tang, T.; Shi, Z. *J. Appl. Polym. Sci.* **2011**, *120*, 1758.
23. Tang, T.; Shi, Z.; Yin, J. *Mater. Chem. Phys.* **2011**, *129*, 356.
24. Silvis, H. C.; White, J. E. *Polym. News* **1998**, *23*, 6.
25. Utracki, L. A. Clay-Containing Polymeric Nanocomposites; Vol. 2, chapter 5; Rapra Technology: Shawbury, **2004**.
26. Fornes, T. D.; Yoon, P. J.; Paul, D. R. *Polymer* **2003**, *44*, 7545.
27. Shas, R. K.; Paul, D. R. *Polymer* **2006**, *47*, 4075.
28. Gurmendi, U.; Eguiazábal, J. I.; Nazábal, J. *Polym. Int.* **2006**, *55*, 399.
29. Vaia, R. A.; Sauer, B. B.; Tse, O. K.; Giannelis, E. P. *J. Polym. Sci. Polym. Phys.* **1997**, *35*, 59.
30. Yu, Z.-Z.; Yan, C.; Yang, M.; Mai, Y.-W. *Polym. Int.* **2004**, *53*, 1093.
31. Yeh, J. M.; Chen, C. L.; Huang, C. C.; Chang, F. C.; Chen, S. C.; Su, P. L.; Kuo, C. C.; Hsu, J. T.; Chen, B. Y.; Yu, Y. H. *J. Appl. Polym. Sci.* **2006**, *99*, 1576.
32. Chang, I. H.; Seo, B. S.; Kim, S. H. *J. Polym. Sci. Polym. Phys.* **2004**, *42*, 3667.
33. Masenelli-Varlot, K.; Reynaud, E.; Vigier, G.; Varlet, J. *J. Polym. Sci. Polym. Phys.* **2002**, *40*, 272.
34. Giannelis, E. P.; Krishnamoorti, R.; Manias, E. *Adv. Polym. Sci. (Polymers in Confined Environments)* **1999**, *138*, 107.
35. González, I.; Eguiazábal, J. I.; Nazábal, J. *Polym. Eng. Sci.* **2006**, *46*, 864.
36. Lee, K. M.; Han, C. D. *Polymer* **2003**, *44*, 4573.
37. Cho, J. W.; Paul, D. R. *Polymer* **2001**, *42*, 1083.
38. Gyoo, P. M.; Venkataramani, D.; Kim, S. C. *J. Appl. Polym. Sci.* **2006**, *101*, 1711.
39. Torre, L.; Lelli, G.; Kenny, J. M. *J. Appl. Polym. Sci.* **2006**, *100*, 4957.
40. González, I.; Eguiazábal, J. I.; Nazábal, J. *Macromol. Mater. Eng.* **2008**, *293*, 781.
41. Ellis, T. S. *Polymer* **2003**, *44*, 6443.
42. Yoo, Y.; Paul, D. R. *Polymer* **2008**, *49*, 3795.
43. Spencer, M. W.; Cui, L.; Yoo, Y.; Paul, D. R. *Polymer* **2010**, *51*, 1056.
44. Cui, L.; Ma, X.; Paul, D. R. *Polymer* **2007**, *48*, 6325.
45. Paul, D. R.; Robeson, L. M. *Polymer* **2008**, *49*, 3187.
46. Chavarría, F.; Paul, D. R. *Polymer* **2004**, *45*, 8501.
47. Goitisolo, I.; Eguiazábal, J. I.; Nazábal, J. *Polym. Adv. Tech.* **2009**, *20*, 1060.
48. Zhong, Y.; Janes, D.; Zheng, Y.; Hetzer, M.; De Kee, D. *Polym. Eng. Sci.* **2007**, *47*, 1101.
49. Kim, D. H.; Fasulo, P. D.; Rodgers, W. R.; Paul, D. R. *Polymer* **2007**, *48*, 5308.
50. González, I.; Eguiazábal, J. I.; Nazábal, J. *Polymer* **2005**, *46*, 2978.
51. Thellen, C.; Orroth, C.; Froio, D.; Ziegler, D.; Lucciarini, J.; Farrell, R.; D'Souza, N. A.; Ratto, J. A. *Polymer* **2005**, *46*, 11716.
52. Shah, D.; Maiti, P.; Gunn, E.; Schmidt, D. F.; Jiang, D. D.; Batt, C. A.; Giannelis, E. R. *Adv. Mater.* **2004**, *16*, 1173.
53. Ray, S. S.; Bousmina, M.; Okamoto, K. *Macromol. Mater. Eng.* **2005**, *290*, 759.